Aircraft 4-D Constant Velocity Control System

Edwin C. Foudriat*
Marquette University, Milwaukee, Wis.

A 4-D system for sequencing of aircraft in a traffic controlled environment is developed. A closed-form approximation for determination of the constant airspeed necessary to fly a fixed ground path consisting of straight line and constant radius arc segments is shown to have accuracy of better than 0.1%. Heading and bank angle required on the turns are also computed. These calculations are used as commands to an aircraft and are periodically updated to provide for elimination of errors accumulated during flight. The concept is capable of being implemented over a broad spectrum of aircraft under active control from those with full RNAV autopilots, to those under radar vector control where commands are relayed verbally from a traffic controller. The system capability is demonstrated in a simulation of a modern transport aircraft with a typical autopilot and auto throttle, navigation information, and computer to process the command equations. Sequencing accuracies within a few seconds are obtained when the aircraft is subjected to combined unsteady winds (gusts) and errors in the knowledge of the steady wind conditions.

I. Introduction

INCREASED capacity of air traffic can be obtained through closer spacing and more precise sequencing of aircraft in both terminal and enroute environments.[1] To be usable this increase must be achieved for a large class of the aircraft under active traffic control, must not jeopardize the safety of the vehicles, and preferably should decrease the workload of the ATC controller.

To improve longitudinal spacing and sequencing, the 4-D control concept has been proposed.[1] Here the aircraft must not only fly a prescribed route and altitude profile (3-D) but must arrive at points along the route at prescribed times (4-D). This paper deals with a method for controlling such flights in the terminal area which should be applicable to a large class of aircraft with a wide variety of IFR navigational instruments on board.

Two techniques for 4-D control, velocity control, and path stretching have been proposed. Path stretching has been studied by Straeter and Park,[3] Erzberger,[2] Dunning, Hemesath et al.,[4] etc. The latter conclude that path stretching will be the primary method in the terminal area based upon the inability of velocity variation without configuration change to appreciably affect flight time. This is true in the terminal area if configuration is established a priori. However, if configuration is selected based upon the consideration of distance and flight time required, then a considerable time variation is available. In addition, path stretching is more difficult for a ground controller to monitor because aircraft are not on the same paths, and aircraft with limited navigational equipment requires more radar vectoring by the traffic controller. Finally, path stretching requires larger areas insensitive to noise, a condition not likely to be available in many critical airports. Undoubtedly both velocity control and path stretching will be used to provide precise control for the aircraft to reach the target point at the prescribed time.

Erzberger and Pecsvaradi,[5] Madden and Desai,[6] and Farrington and Goodson,[7] have considered 4-D velocity control concepts. Basically, all have assumed paths consisting of straight-line segments and constant radius turns. In such systems the major problem is accounting for the steady winds on the turns. Madden and Desai indicate the use of a psuedo-waypoint to make the trajectory "flyable." They employ a feed-forward system based upon an onboard model computation and control the aircraft to the model state. They indicate since a constant airspeed is specified, that path synthesis also involves some path stretching in order to meet the elapsed-time constraint.

Erzberger and Pecsvaradi, using a trajectory consisting of straight lines and constant radius turns, derive a constant airspeed based upon the first-order approximation algorithm for combining airspeed and wind speed to fly the trajectory in the prescribed time. Using the constant airspeed, a reference or target position is generated along the trajectory and the actual aircraft is controlled to fly the target position. Farrington and Goodson[7] use a similar procedure except that they use the complete equation based upon the elliptic integral solution. They also consider linear optimal digital autopilots by which the aircraft "flies wing" on the reference point moving along the trajectory.

This paper considers an approach to 4-D control which does not force the aircraft to fly to a moving target. Instead the constant airspeed necessary to complete the remaining portion of the desired trajectory in the remaining time alotted is calculated and used as the command for the longitudinal autopilot (autothrottle) or the pilot. The paper discusses the algorithm developed to make this calculation without solution of the incomplete elliptic equation and demonstrates the capability of the resultant iterative approach. This concept is tested using a digital simulation of the horizontal motion of modern transport aircraft equipped with typical longitudinal and lateral autopilot systems. The simulation demonstrates the ability of the velocity-command controller to bring the airplane to the desired terminal conditions considering the effect of gusts and errors in the knowledge of prevailing wind conditions.

II. An Algorithm for Determination of Constant Airspeed

The desired ground trajectory in the horizontal plane consists of straight-line segments and connecting circular arcs of constant radius† as shown in Fig. 1. It is desired to determine the time necessary to fly the ith straight-line and circular-arc segments based on the airspeed v_u.

Received November 26, 1973; revision received March 26, 1974. This work is partially supported by the NASA-ASEE Summer Faculty Fellowship Program of Langley Research Center and Old Dominian University.

Index categories: Aircraft Navigation, Communication, and Traffic Control; Aircraft Flight Operations.

*Associate Professor, Dept. of Electrical Engineering.

†The radius R is usually selected based upon maximum operating velocity during the flight regime of interest and maximum bank angle considering passenger comfort.

The time to fly the ith straight-line portion is

$$t_i = \text{time to fly } i\text{th straight-line segment} = d_i/v_g$$

where d_i = distance and v_g = ground velocity.

The ground velocity v_g can be calculated from

$$v_g = v_g(\cos\alpha_i, \sin\alpha_i) = v_u + v_w$$
$$= v_u(\cos\psi_i, \sin\psi_i) + v_\omega(\cos\psi_\omega, \sin\psi_\omega) \qquad (1)$$

where $\boldsymbol{v}_\mu$ = airspeed vector and $\boldsymbol{v}_\omega$ = wind speed vector. Solving for v_g gives

$$v_g = v_u\{1 + k^2 + 2k\cos(\psi_i - \psi_\omega)\}^{1/2} \qquad (2)$$

where $k = (v_\omega/v_u)$.

Since variable α_i (the ground heading of the ith segment) is independent of flight conditions, Eq. (2) should be rewritten, eliminating ψ_i. Manipulating Eq. (1) gives

$$\cos(\psi_i - \psi_\omega) = (v_{g_i}/v_u)\cos(\alpha_i - \psi_\omega) - k \qquad (3)$$

Upon substitution of Eq. (3) in Eq. (2) and after further algebraic manipulation, the result is

$$v_g = v_u\{[1 - k^2\sin^2(\alpha_i - \psi_\omega)]^{1/2} + k\cos(\alpha_i - \psi_\omega)\} \qquad (4)^\ddagger$$

Based on Eq. (4), the time to traverse the ith segment is

$$t_i = d_i/[v_u\{(1 - k^2\sin^2(\alpha_i - \psi_\omega))^{1/2} + k\cos(\alpha_i - \psi_\omega)\}] \qquad (5)$$

To determine the time to fly the ith circular arc segment, consider the instantaneous position of the aircraft relative to the ith arc center as

$$x = R(-\sin\alpha, \cos\alpha)$$

where R = the radius and α = instantaneous heading on the arc.

The aircraft ground velocity is

$$\dot{x} = v_g = \omega \times x = (\dot{\alpha}R\cos\alpha, \dot{\alpha}R\sin\alpha)$$

From Eq. (1), $\mathbf{v}_g = v_g(\cos\alpha, \sin\alpha)$. Hence

$$\dot{\alpha} = v_g/R \qquad (6)$$

Using Eq. (4), Eq. (6) can be written as

$$\int_0^{t_i'} v_u/R\,dt$$
$$= \int_{\alpha_i}^{\alpha_{i+1}} d\alpha/[(1 - k^2\sin^2(\alpha - \psi_\omega))^{1/2} + k\cos(\alpha - \psi_\omega)] \qquad (7)$$

Since the left-hand side of Eq. (7) is constant, the time to fly the ith circular arc is given as

$$t_i' = R/v_u\int_{z_i}^{z_{i+1}}[(1 - k^2\sin^2 z)^{1/2} - k\cos z]/(1 - k^2)dz \qquad (8)$$

where $z = \alpha - \psi$.

The first term of Eq. (8) is the well-known incomplete elliptic integral of the second kind. Using the approximation

$$(1 - x)^{1/2} \approx 1 - (x/2) - (x^2/8)$$

the integral can be evaluated as

$$t_i' \approx R/v_u(1 - k^2)\{(1 - k^2/4 - 3/32k^4)z - k\sin z$$
$$+ 1/8(k^2 + k^4/4)\sin 2z - k^4/256\sin 4z\}\Big|_{z_i}^{z_{i+1}} \qquad (9)$$

Equations (5) and (9) can be combined to calculate the flight time for the fixed ground path at constant airspeed as

‡Note that Erzberger[5] uses the $0(k)$ approximation for Eq. (4).

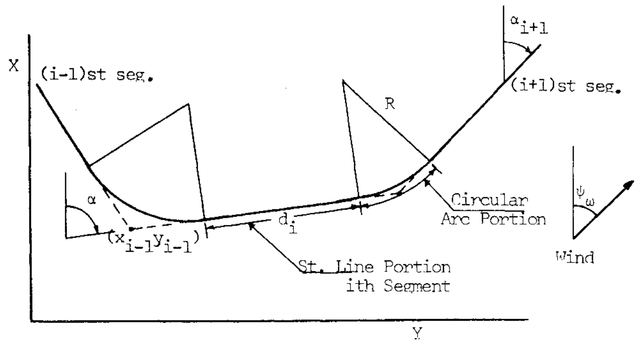

Fig. 1 Sketch of ith trajectory segment.

$$T_D = 1/v_u\sum_i d_i/f_1(k, z_i) + Rf_2(k, z_{i+1}, z_i) \qquad (10)$$

where f_1 is the denominator term of Eq. (5) and f_2 is the right-hand side of Eq. (9). For the problem considered, T_D is given and v_u is required. It will be shown in Sec. IV that v_u can be readily determined iteratively by

$$v_u^{(k+1)} \approx \sum_i 1/T_D(d_i/f_1(k^{(k)}, z_i) + Rf_2(k^{(k)}, z_{i+1}, z_i)) \qquad (11)$$

where $k^{(k)}$ indicates the kth iterative solution; that is,

$$k^{(k)} = v_\omega/v_u^{(k)}$$

III. Determination of Heading and Bank Angle

The previous equations can be used to determine the precise aircraft heading angle required to flight the straight-line portions of the trajectory and the bank angle needed to fly the constant radius turns. The heading angle is solved from Eqs. (3) and (4) as

$$\psi_i = \cos^{-1}\{[(1 - k^2\sin^2 z_i)^{1/2}$$
$$+ k\cos z_i]\cos z_i - k\} + \psi_\omega \qquad (12)$$

where $z_i = \alpha_i - \psi$.

The bank angle can be calculated with the coordinated turn equation

$$\Phi = \tan^{-1}\left(\frac{v_u\dot{\psi}}{g}\right) \qquad (13)$$

by differentiating for $\dot{\psi}$ in Eq. (12)

$$-\dot{\psi}\sin(\psi - \psi_\omega) = -\dot{z}\sin z\{(1 - k^2\sin^2 z)^{1/2} + 2k\cos z$$
$$+ k^2\cos^2 z/(1 - k^2\sin^2 z)^{1/2}\}$$

Solving for $\dot{\psi}$ and noting that z can be obtained from Eq. (6) gives

$$\dot{\psi} = v_u/R\sin z\{(1 - k^2\sin^2 z)^{1/2} + k\cos z\}\cdot$$
$$\{(1 - k^2\sin^2 z)^{1/2} + 2k\cos z$$
$$+ k^2\cos^2 z/(1 - k^2\sin^2 z)^{1/2}\}/\sin(\psi - \psi_\omega) \qquad (14)$$

Equation (12) can be used for control during the straight line segment of flight and Eqs. (13) and (14) used to command the aircraft on the turns.

IV. Constant Velocity Terminal Controller System—Command Processor

The block diagram, Fig. 2, shows the terminal controller concept utilizing the constant velocity command system. The controller consists of three parts: 1) the autopilot system which provides lateral and vertical steering to maintain the path and an autothrottle to maintain commanded velocity, 2) the navigation system which determines the aircraft position relative to the commanded path, and 3) the command processor which provides the

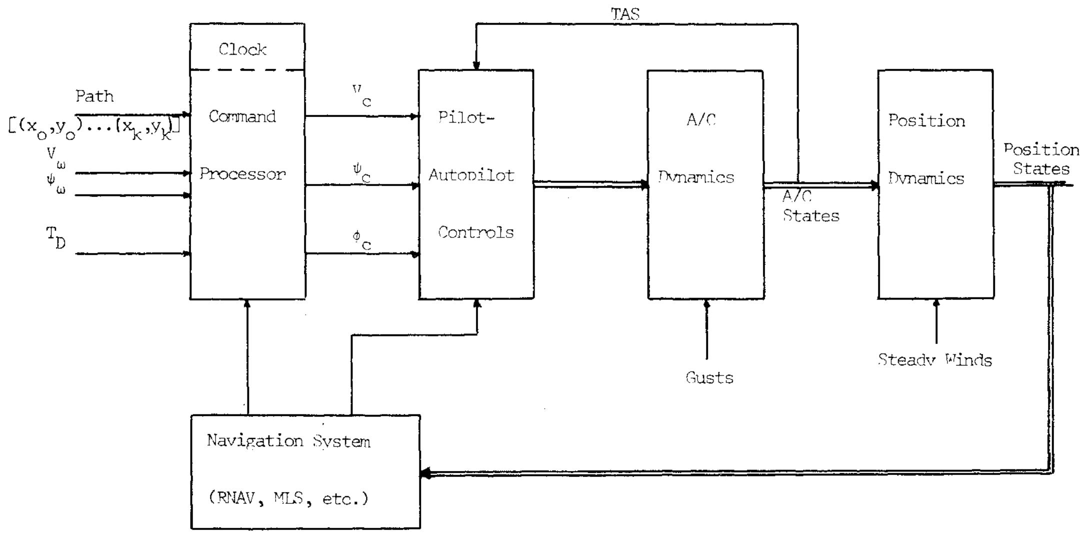

Fig. 2 Block diagram of 4-D constant velocity terminal controller.

Table 1 Error between expansion integral and elliptic integral function

Angle, °/k	0.1736	0.4226	0.6428	0.9659
30	—	-4.41×10^{-7}	-5.758×10^{-6}	-7.153×10^{-5}
60	-1.428×10^{-7}	-3.196×10^{-5}	-4.393×10^{-4}	-6.911×10^{-3}
90	-8.553×10^{-7}	-1.94×10^{-4}	-2.832×10^{-3}	-6.391×10^{-2}

signals necessary to fly the path in the desired time. The basic problems investigated in this study are the capability of the command processor to generate the desired command signals based upon the equations developed in Sec. II and III and the ability of the combined command processor-autopilot to successfully accomplish the flight when realistic disturbances exist. This section will consider the characteristics of the command processor system. Following this, results of a simulator study will be discussed to indicate the system capability to execute the commanded flight.

The command processor is required to take the path indicated by a sequence of (x,y) coordinate points and generate: 1) a "flyable" trajectory; 2) the constant velocity necessary to fly that trajectory in time T_D based upon estimates of the steady wind magnitude v_ω and direction ψ_ω based upon Eq. (11); and 3) the desired heading angle ψ_i on each straight-line segment and bank angle Φ during each turn, using Eqs. (12) and (13)–(14), respectively.

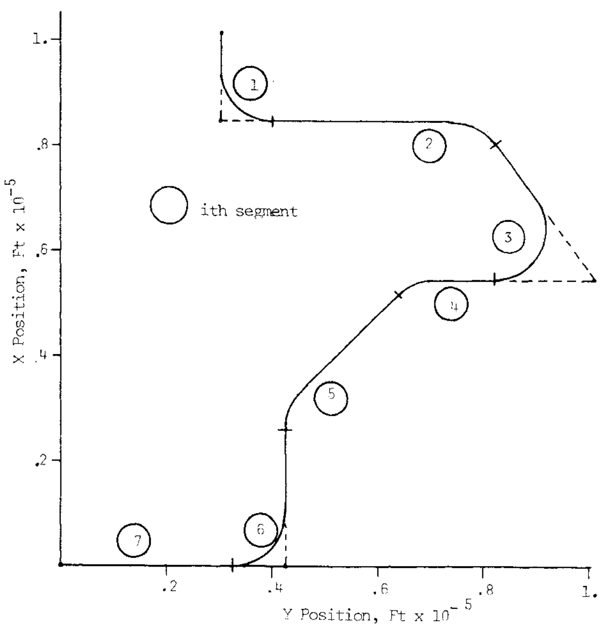

Fig. 3 Convergence test trajectory.

Flyable Trajectory Processor

The flyable trajectory generator takes the sequence of (x_i,y_i) points which indicate the path and fits constant radius arcs between straight-line segments as indicated in Fig. 1. The ground-path angle on each straight-line segment is obtained by

$$\alpha_i = \tan^{-1}((y_i - y_{i-1})/(x_i - x_{i-1}))$$

The straight-line distance for each segment of the "flyable" trajectory to be used in Eq. (11) is

$$d_i = [(x_i - x_{i-1})^2 + (y_i - y_{i+1})^2]^{1/2} - R[|\tan\alpha_i/2| + |\tan\alpha_{i-1}/2|]$$

Constant Velocity Processor

In analyzing the constant velocity processor Eq. (11), two questions need to be considered; first, how adequate is the expansion for $(1-x)^{1/2}$ when terms beyond (x^2) are ignored and second, will the simple iterative procedure, where the previous estimate of v_u is used for k, converge rapidly and accurately?

Table 1 indicates the error between the expansion integral and the correct value for the Elliptic-Integral Function for angles up to 90°. For realistic values of k (wind < 50% of airspeed), the error for turns up to 90° is insignificant, being only 0.019%. Turns larger than 90° were not tested because the results indicating accuracy using the expansion seemed more than adequate.

The convergence question was investigated by determining the number of iterations necessary before the velocity change became insignificant. For this study the test-trajectory sketched in Fig. 3, considered more complex than most normal approach paths, was used.

Conditions for the trajectory of Fig. 3 were $T_D = 720$ sec, $v_\omega = 33.75$ fps, and $\psi_\omega = 0.°$ The initial value, $k^{(o)} = 0$. Table 2 indicates that the simple iterative scheme provides rapid convergence. In using Eq. (11) with other

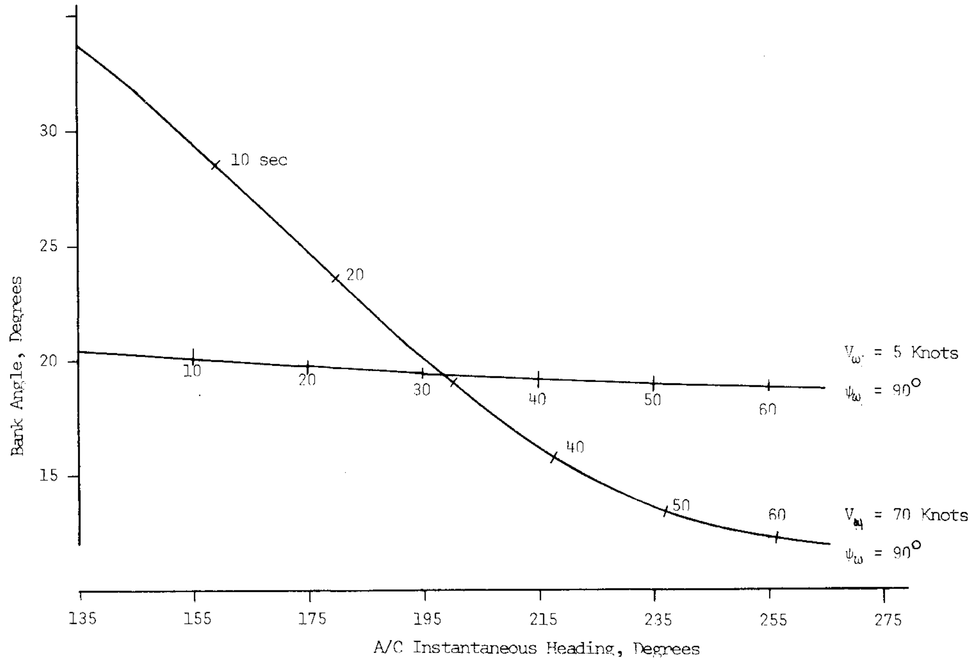

Fig. 4 Bank angle on 3rd turn of trajectory in Fig. 3.

paths, winds, and times, no convergence problems were experienced.

Heading and Bank Angle Processor

The processor is capable of determining the aircraft heading angle during the straight-line portions of the flight and the bank angle necessary to fly a constant-ground radius turn at constant airspeed when a steady wind exists. The heading angle calculation is straightforward and therefore will not be discussed. However, the bank-angle command from Eq. (13) and (14) shows some interesting results.

Figure 4 shows the bank angle required to complete turn 3 of the trajectory Fig. 3, for two widely differing wind speeds. The bank angle is shown as a function of the instantaneous ground heading of the aircraft. It is noted that bank angle is always a minimum when the plane is heading directly into the wind and a maximum where heading with the wind. For large relative wind speeds, the bank angle can change significantly over a large turn. Figure 4 includes time points on the curves which indicate time after initiation of the turn. They show that changes occur at a rate that the pilot or autopilot system can easily follow.

These results indicate that the command processor system is capable of developing a flyable trajectory from a sequence of coordinate points, determining the constant airspeed necessary to execute that trajectory in a commanded time when the steady wind condition is known and then can provide the autopilot, heading, and turn command needed to fly the desired trajectory.

V. Constant Velocity Terminal Controller System—Flight Simulation

A study was conducted to determine the capability of the constant velocity command processor to function in conjunction with a typical autopilot to direct an aircraft over the desired trajectory in the commanded time and to ascertain the affects of wind disturbances and other uncertainties.

With the command processor, there are many methods by which a flight system could be implemented. For example, the sophisticated technique of generating a moving point along the trajectory and controlling the aircraft to that point could be implemented. This concept was studied by Erzberger and Farrington using optimal autopilots. Alternatively, one might use the processor to generate voice instructions to the pilot in a manner compatible with present ATC radar vectoring. The commands would indicate aircraft heading including crab angle, required airspeed, the times to initiate turns, and the bank angle needed in each turn in units acceptable to the controlled aircraft. Periodically the commands would be updated to correct for errors, drifts, and disturbances.

Table 2 Iteration needed for convergence of constant airspeed (Eq. 11)

Velocity change Less than—fps	Iterations
0.5	4
0.05	4
0.005	5
0.0005	6

In this study, a system between these two extremes was investigated. It was assumed that the aircraft possessed an RNAV or MLS system capable of determining aircraft position and an autopilot. These systems as indicated in Fig. 2 were used in conjunction with the command processor to generate signals to flight the aircraft over the desired trajectory. In the following subsections, the autopilot and navigation system configurations will be discussed briefly and the simulation results presented.

Simulation Study Dynamics

Aircraft

The aircraft was simulated using point mass dynamics relative to the steady air mass for its longitudinal and lateral axis. It was assumed to fly at constant altitude so vertical dynamics were neglected. Dynamic pressure was calculated using instantaneous airspeed including gusts but the effect of velocity on the stability and engine thrust coefficients was ignored. The lateral point mass equation included bank angle to change heading in a constant altitude turn. Bank angle was computed using simple roll dynamics. Yaw dynamics and any yaw coupling into the roll axis was neglected. The mass, inertia, and

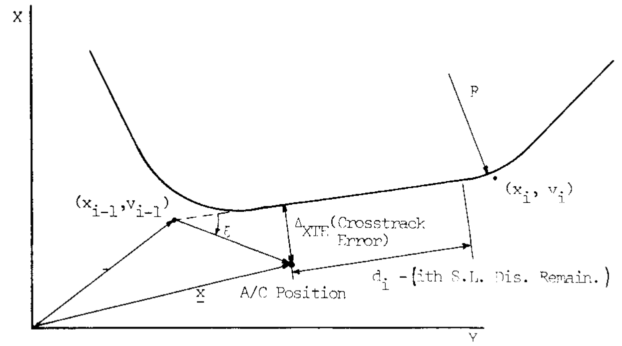

Fig. 5. Relation of aircraft position to *i*th trajectory segment.

c.g. of the aircraft were assumed constant. The coefficients selected were for a modern jet transport at 5000 ft with a velocity of 193 knots.

The dynamic equations included the effect of the steady-state winds in determining the motion of the aircraft with respect to the fixed, flat earth. Gusts were incorporated in the longitudinal and lateral axes using the standard rational Dryden model. Because of the point mass nature of the lateral dynamics assumed for the aircraft, the lateral gust velocity was input into a linear sideforce equation before its affects were added to the aircraft's lateral motion. The gust affects on heading deviation were ignored. The longitudinal gusts were added directly to the aircraft velocity to obtain instantaneous true airspeed and dynamic pressure.

Navigation System

The navigation system was assumed ideal in that the position of the aircraft was known without error or lag whenever needed for the command processor or the autopilot. The aircraft position was used to determine the aircraft crosstrack deviation and along-track position on the *i*th segment, as shown in Fig. 5. The crosstrack deviation was used as the input error signal to the lateral autopilot to maintain the aircraft on the trajectory. The along-track position was used periodically by the command processor to recalculate the constant velocity required during the remaining period of the flight in order to attain the final position and to determine when the aircraft should initiate the commanded bank to begin each turn. Turns were flown "open" loop using commanded bank angle. No crosstrack error correction or new velocity commands were processed by the controller during turns.

Autopilot

The autopilot block diagrams for the lateral and auto throttle system are shown in Fig. 6a and 6b. The lateral autopilot contains two modes; a bank angle command inner loop and crosstrack error control outer loop. The latter was used during the straight-line portions of the flight only. Limiters were used on aileron authority and bank angle command in order to provide more realistic aircraft dynamics.

Either heading error or crosstrack error rate can be used in the outer lateral loop to provide stability. With accu-

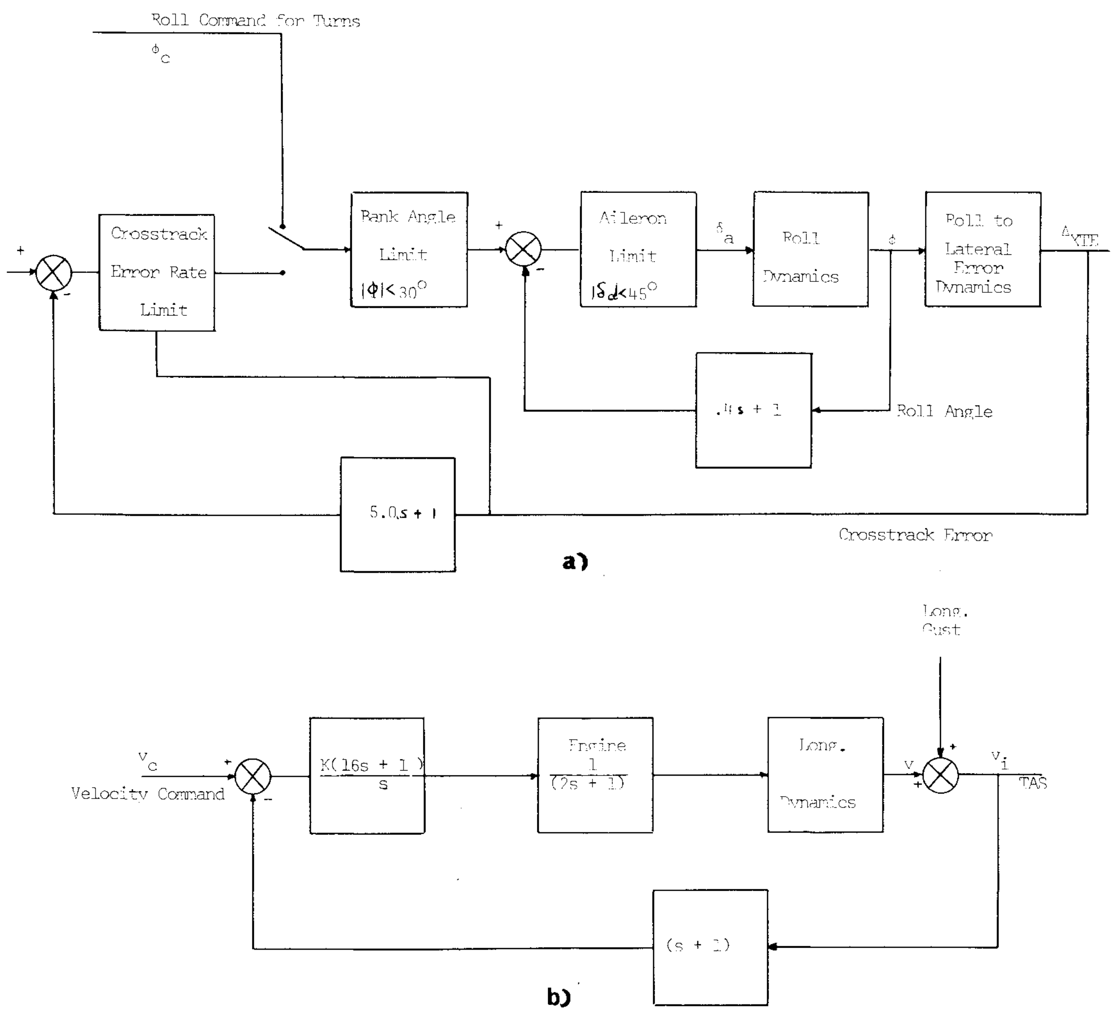

Fig. 6 Autopilot. a) Lateral system. b) Autothrottle system.

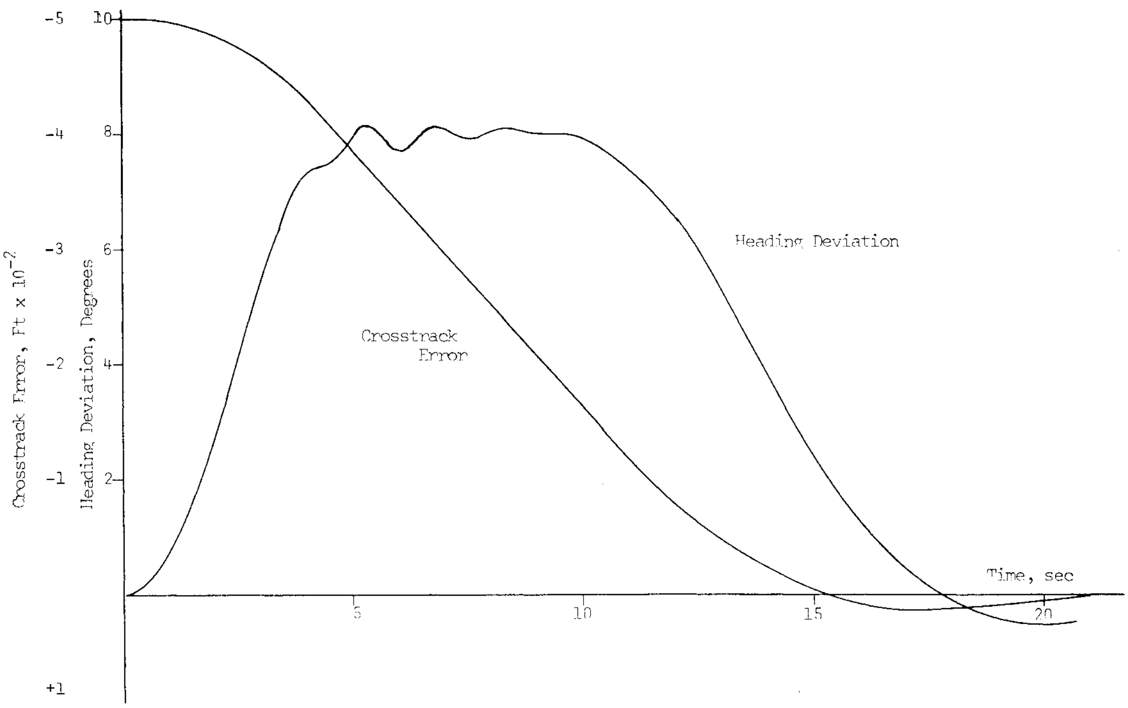

Fig. 7 Typical lateral autopilot response.

rate wind knowledge, they are equivalent. However, errors in the steady-state wind lead to lateral offset if heading error is used. Hence crosstrack error rate was selected. In most autopilots a combination is used: washed out heading error for the high-frequency deviation and differentiation of crosstrack error for the low-frequency deviation. The lateral autopilot outer loop also included a limiter to restrict the crosstrack error rate in order to reduce overshoot. In design of the autopilot, nominal gains were chosen. The response of the lateral autopilot to an initial 500 ft deviation is shown in Fig. 7.

The autothrottle system is shown in Fig. 6b. The integrator in the forward loop was used to eliminate the steady-state error. Filtering was not used on the TAS signal to reduce the affect of gusts, although such filtering would provide a smoother operating autothrottle and improve somewhat the system's ability to maintain the desired ground speed.

Simulation Study Results

The study was designed to determine the ability of the constant velocity command processor when employed with a nominal autopilot system to provide 4-D control. In this simulation the constant velocity command was reinitialized periodically. As a result, aircraft position was not continually controlled at all points along the trajectory, but only as a result of the final position-elapsed time constraint. Perturbing affects considered were lateral and longitudinal gusts and inaccurate data on steady wind heading and velocity.

Table 3 indicates the error in position at the final time for the trajectory shown in Fig. 8. The desired flight time for the trajectory was 680 sec. Cases I and II have different noise sequences. The final position errors indicate the ability of the controller to provide arrival accuracies within one second for reasonable error and disturbance conditions. Similar results were obtained for other trajectories and other conditions. From these studies one can conclude under nominal error conditions that 4-D sequencing control to within a few seconds in the terminal area is reasonable.

The study also determined the capability of the lateral command and control loop to maintain the aircraft on the command trajectory. Lateral error for Case II, as shown in

Table 3 Terminal position error for 4-D constant velocity terminal controller

Case	Conditions Assumed	Conditions Actual	Position error (at t = 680 sec)
I	V_ω = 30 fps, ψ_ω = 90°	V_ω = 30 fps, ψ_ω = 90°, σ_ω = 5 fps	+38.09 ft
II	V_ω = 30 fps, ψ_ω = 0°	V_ω = 30 fps, ψ_ω = 0°, σ_ω = 5 fps	−75.37 ft
III	V_ω = 30 fps, ψ_ω = 120°	V_ω = 30 fps, ψ_ω = 90°, σ_ω = 5 fps	−139.6 ft
IV	V_ω = 35 fps, ψ_ω = 90°	V_ω = 30 fps, ψ_ω = 90°, σ_ω = 5 fps	+268.56 ft

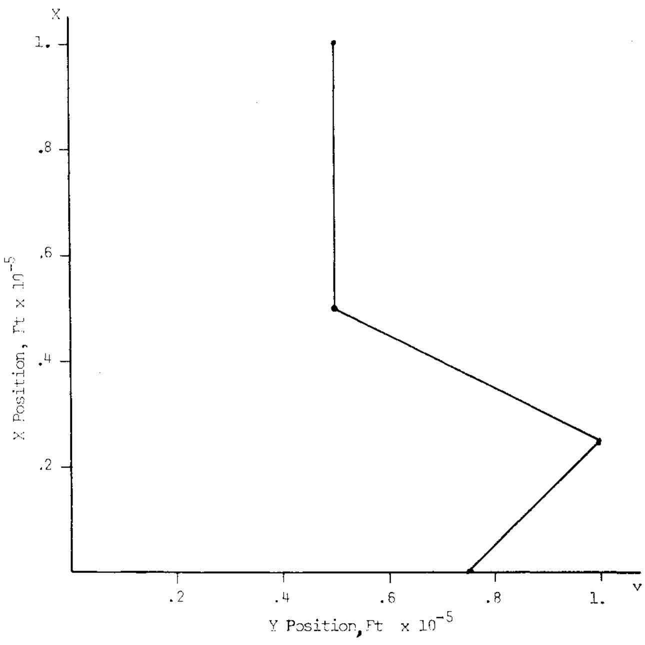

Fig. 8 Test trajectory for simulation studies.

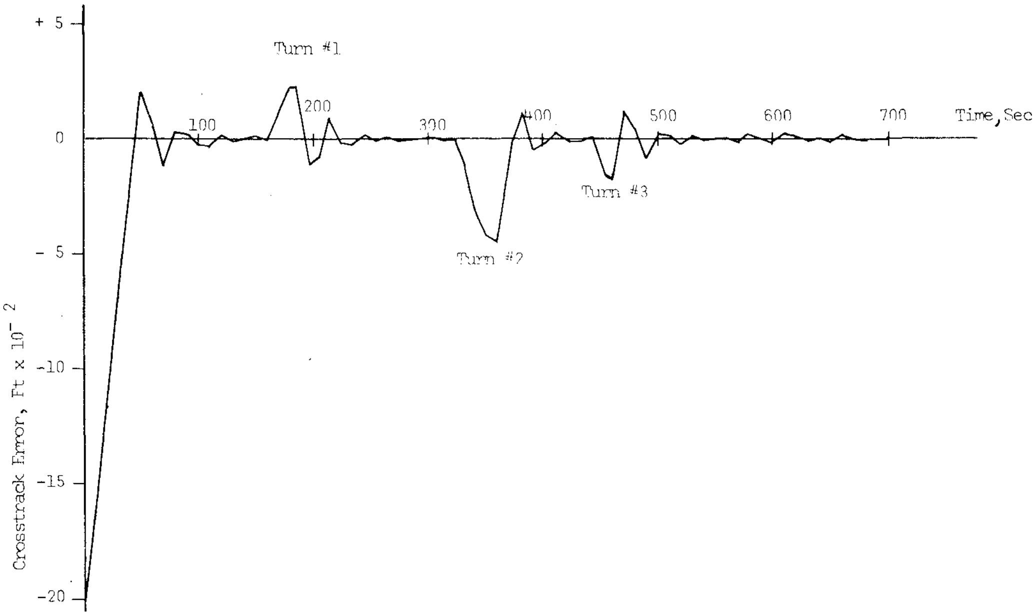

Fig. 9 Crosstrack error in Case 2.

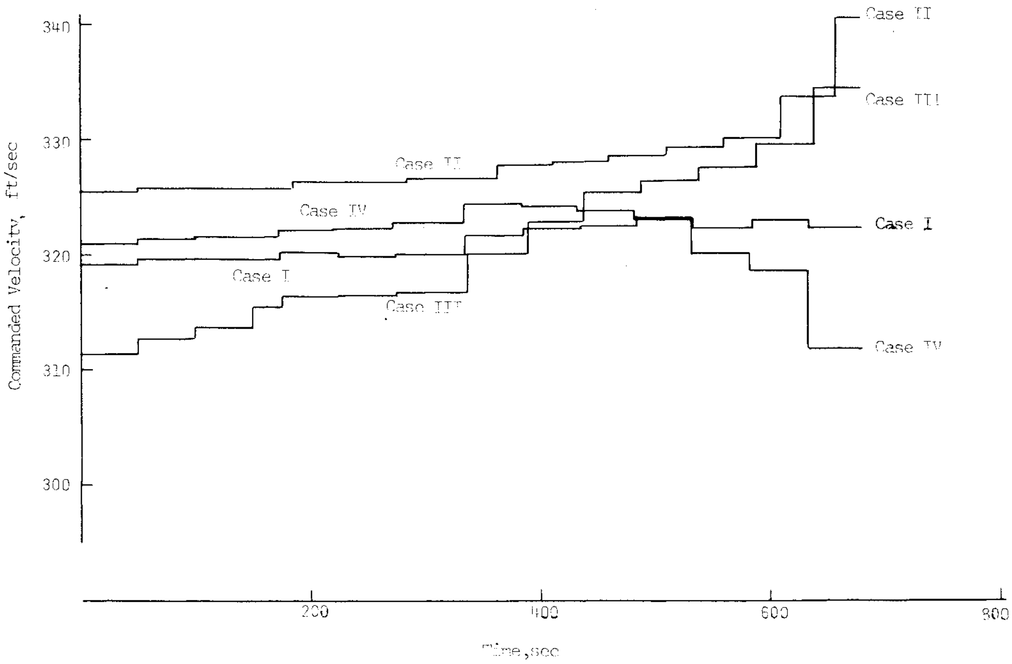

Fig. 10 Commanded velocity for Cases 1-4.

Fig. 9, is typical. The initial position error is −2000 ft. After the initial transient, the crosstrack error variations are due to the lateral gust and the error generated during the three turns as indicated on Fig. 9.

The turn errors are caused because the autopilot has no anticipation built into the command loop. Madden[6] shows that by commanding the bank somewhat early, much of this error can be eliminated. However, the error should cause no trouble unless there are close parallel routes where overshoot becomes critical. In this case it becomes necessary to either establish identical procedures for all turning aircraft or to shift the (x,y) coordinates of the turning point to reduce any overshoot penetration problems. The feature that makes the commanded bank using constant airspeed and estimates of wind conditions desirable is uniformity. By compensating for winds, the remaining source of error becomes the turn initiation which is more predictable and hence more easily compensated by procedure or route planning.

Figure 10 shows the commanded velocity variations for Cases I–IV of Table 3. For conditions where knowledge of the steady winds are correct, changes in velocity are usually small. Case II has been included because the wind gust tended to slow the aircraft ground speed for an extended period between 500–600 sec, resulting in a 10 fps increase in velocity command over the final 100 sec of the flight. Even so, the aircraft was only 75 ft from the target point. The increase in commanded velocity at about 350 sec for all cases is mainly a result of the turn error and lateral course correction which reduces the along track velocity component during correction. The velocity corrections where wind conditions are in error remain reasonable and, as expected, occur mainly during the final portion of the flight.

For Cases I–IV, velocity commands were calculated at 50 sec intervals. Velocity·command charges occurring during a turn were ignored until the turn was completed. At that point, the velocity command was recalculated and used for the next 50 sec interval. A few runs were made to determine the effect of a 20 sec reinitialization rate. For the runs studied, the commanded velocities were substantially the same and differences in final position were only a few feet less than runs with the longer update interval. For trajectories and conditions tested, update rates approximately once per minute appear reasonable in order to attain arrival accuracies within a few seconds.

VI. Conclusions

The study indicates that a constant velocity controller system is an entirely feasible method for accomplishing 4-D aircraft control on a terminal or enroute environment. The command processor system is shown to provide an accurate solution to the velocity, heading, and bank angle commands. The system equations appear to be simple enough to implement on a small general-purpose airborne digital computer or to be solved as an adjunct to the ground controller's data processing and voice commands relayed to the pilot during radar vectoring instructions.

The simulation study indicates that for an aircraft with a typical autopilot and autothrottle, open-loop velocity control with refresh rates of approximately 1 min are adequate to accomplish sequencing accuracies in the order of a few seconds even when gusts and realistic errors in knowledge of the steady winds exist. Errors of this magnitude should significantly improve sequencing accuracy in terminal traffic control.

The results show that the utilization of programed bank angles based upon assumed steady winds significantly reduces dispersion on constant ground radius turns. The remaining dispersion is a result of procedure in execution and can be made acceptable by procedural standardization or route planning.

In this paper, the constant velocity terminal controller is demonstrated for a typical autopilot system. Its greatest asset, however, appears to be the wide class of systems for which it can be implemented. Further studies should be conducted to determine the accuracy capability for final control for other members of this class in order that an improved sequencing system be made available for air traffic control.

References

[1]"Application of Area Navigation in the National Airspace System," Rept. by FAA/INDUSTRY RNAV Task Force, April 1973, FAA, Washington, D.C.

[2]Erzberger, H. and Lee, H. G., "Terminal Area Guidance Algorithm for Automated Air Traffic Control," TN-D-6773, April 1972, NASA.

[3]Straeter, T. and Park, S., "Near Terminal Area Optimal Sequencing and Flow Control as a Mathematical Programming Problem," presented at the Mathematical Programming Society, Symposium on Nonlinear Programming, March 1973, George Washington University, Washington, D.C.

[4]Dunning, K., Hemesath, N. et al., "Curved Approach Path Study," Rept. DOT-FA72WA-2824, Oct. 1972, Collins Radio Co.,

[5]Erzberger, H. and Pecsvaradi, T., "4-D Guidance System Design with Application to STOL Air Traffic Control," presented at the 1972 Joint Automatic Control Conference, Paper 14-1, Aug. 1972, Stanford University, Stanford, Calif.

[6]Madden, P. and Desai, M., "Nonlinear Trajectory—Following and Control Techniques in the Terminal Area Using the Microwave Landing System Navigation Sensor," Contract DOT-TSC-551, 1973, Charles Stark Draper Lab., MIT, Cambridge, Mass.

[7]Farrington, F. and Goodson, R., "Simulated Flight Tests of a Digitally Autopiloted STOL-Craft on a Curved Approach with Scanning Microwave Guidance," presented at the 1973 Joint Automatic Control Conference, Paper 15-2, June 1973, Ohio State University, Columbus, Ohio.

JUNE 1974 J. AIRCRAFT VOL. 11, NO. 6

Stability and Control of Hingeless Rotor Helicopter Ground Resonance

Maurice I. Young* and David J. Bailey†
University of Delaware, Newark, Del.

The ground resonance instability of advanced helicopters employing hingeless rotors is examined on a broad parametric basis and a variety of conditions affording inherent stability are determined. Moderate levels of blade internal structural damping in conjunction with typical landing gear damping and stiffness characteristics are shown to be highly effective. This is shown to be a consequence of the offsets of the virtual flapping and lead-lag hinges together with the tuning of the elastically flapping and lead-lagging blades of a hingeless rotor system. Size and scale effects are also included by examining aerodynamically scaled designs which range in gross weight from 5,120 to 48,000 lb. Closed-loop stabilization of the ground resonance instability is considered by using a conventional helicopter swash-plate-blade cyclic pitch control system in conjunction with roll, roll rate, pitch, and pitch rate sensing. This also is shown to be highly effective due to the enormous control power inherent in the advanced hingeless rotor blade designs compared to that of the freely flapping, conventional rotors.

Received June 13, 1973; revision received April 8, 1974. Acknowledgment is made of the support of the U.S. Army Research Office, Durham, N.C., under Grant DA-ARO-D-31-1247G112. Based on a Master of Mechanical and Aerospace Engineering thesis by D. J. Bailey, prepared under the supervision of M. I. Young.

Index categories: Aircraft Handling, Stability, and Control; Aircraft Vibration; Aeroelasticity and Hydroelasticity.

*Professor of Mechanical and Aerospace Engineering. Associate Fellow AIAA.

†Graduate Student and Research Assistant, currently U.S. Army Transportation Engineering Agency, Fort Eustis, Va.

Nomenclature

C_e = landing gear equivalent viscous damping coefficient, lb/ft/sec
C_s = pneumatic shock strut viscous damping coefficient, lb/ft/sec
C_t = tire viscous damping coefficient, lb/ft/sec
CG = helicopter center of gravity
I_x = moment of inertia about x axis, slug-ft^2
K_e = landing gear equivalent spring rate, lb/ft
K_s = non-linear, pneumatic shock strut spring rate, lb/ft
K_t = tire spring rate, lb/ft
M = mass of helicopter